Supporting Information

Laan *et al.* 10.1073/pnas.0710311105

SI Methods

Axoneme Characterization Using Video-Enhanced DIC Microscopy. Coverslips and microscope slides were cleaned in chromosulfuric acid. A 20-μl flow cell was constructed by drawing two parallel lines of vacuum grease ≈5 mm apart on a clean microscope slide and mounting a clean coverslip on top. A solution of axonemes in MRB80 (80 mM K-Pipes, 4 mM $MgCl_2$, 1 mM EGTA, pH 6.8) was flown in and incubated for 5 min to let axonemes adhere to the glass surfaces. The concentration of the axonemes was tuned such that after preparation of the sample approximately five axonemes could be seen in a field of view of the microscope (35×25 μm^2). Axonemes that did not stick to the surface were washed out by washing with two flow cell volumes of MRB80. The flow cell was blocked with 5 mg/ml BSA in MRB80 for 5 min. Afterward, the tubulin mix (10–25 μM tubulin, 5 mg/ml BSA, 1 mM GTP in MRB80) was introduced and the sample was sealed.

Samples were observed on an inverted microscope (DMIRB; Leica Microsystems) with a 100×1.3 N.A. oil-immersion objective by video-enhanced differential interference contrast (VE-DIC) microscopy. The temperature in the sample was adjustable by a sleeve around the objective lens, which was controlled by thermoelectric coolers (Melcor). Images were recorded by a CCD camera (CF8/1, Kappa) and sent to an image processor (Argus 20; Hamamatsu). The resulting image stream was both recorded on a DVD and digitized online at a rate of 1 frame every 2 sec. The number of MTs per axoneme was visually counted. The end of the axoneme with the most and longest MTs was considered the plus-end. For a few conditions, this was confirmed with kinesin-coated beads that walk on the axoneme to the plus-end. Per condition, at least 20 axonemes were counted.

Simulations: Force Dependence and Choice of Parameters. For simulations corresponding to our experiments, the number of nucleation sites was chosen to be nine. The nucleation rate was estimated from the experimentally observed number of MTs per axoneme by using DIC microscopy. It was assumed that in the experiments, steady state was not reached yet, because most experiments were done in the first 5–10 min. The nucleation rate (4.10^{-3} s^{-1}) was chosen so that the number of MTs was the same in experiments and simulation at this time point. v_g in the absence of force was taken from experiments on freely growing MTs under the same conditions (2.5 μm/min). Shrinkage is much faster than growth *in vitro*, so v_s was taken as infinite. We assumed for practical purposes that a force f encountered by an individual MT changed its growth velocity in the following way: $v_g(f) = C_1 \exp(-C_2 f) - C_3$ (1). The constants were estimated from $v_g(0)$ and the apparent stall force for one MT in our experiments (2.7 pN), and by taking C_2 from previous measurements (1.2 pN^{-1}) (1). Note that Brownian ratchet-type theoretical models in fact predict slightly different functional forms for this force–velocity curve (2, 3). We assumed that the individual catastrophe time increases linearly with v_g with a small offset for $v_g = 0$ as previously measured (4). For growth velocities smaller than zero, which can occur when the force encountered by a growing MT suddenly rises above the stall force, T_c was chosen to scale with $1/v_g$. For simulations of bundle oscillations, we modified the following parameters. (*i*) We assumed 15 nucleation sites, because the number of MTs at the kinetochore varies from 10 to 45 (5). (*ii*) We set both v_s and $v_g(0)$ to the same value (2.0 μm/min), because growth and shrinkage velocities are similar in magnitude *in vivo*. Shrinkage was assumed to be force-independent. (*iii*) We increased the catastrophe rate by a factor of 12, because *in vivo* MTs are more dynamic (6). (*iv*) We used a constant small force of 2.6 pN and then varied the nucleation rate until we could near-quantitatively reproduce the oscillatory behavior observed for chromosome oscillations (Fig. 4*A*). For Fig. 4*C*, a smaller number of MTs (six) and a higher force (7 pN) were used.

1. Dogterom M, Yurke B (1997) Measurement of the force-velocity relation for growing microtubules. *Science* 278:856–860.
2. van Doorn GS, Tanase C, Mulder BM, Dogterom M (2000) On the stall force for growing microtubules. *Eur Biophys J* 29:2–6.
3. Mogilner A, Oster G (1999) The polymerization ratchet model explains the force-velocity relation for growing microtubules. *Eur Biophys J* 28:235–242.
4. Janson ME, de Dood ME, Dogterom M (2003) Dynamic instability of microtubules is regulated by force. *J Cell Biol* 161:1029–1034.
5. Rieder CL, Salmon ED (1998) The vertebrate cell kinetochore and its roles during mitosis. *Trends Cell Biol* 8:310–318.
6. Desai A, Mitchison TJ (1997) Microtubule polymerization dynamics. *Annu Rev Cell Dev Biol* 13:83–117.

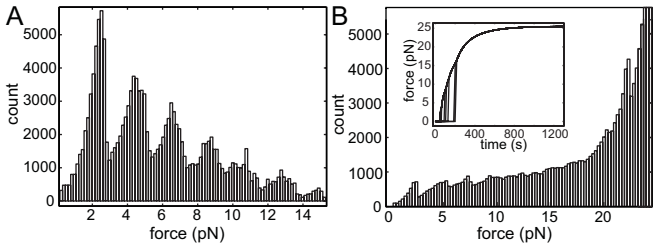

Fig. S1. (*A*) Histogram obtained by adding simulated force traces generated by a GTP bundle for a relatively high catastrophe rate (10 times higher than for the simulation in Fig. 3). The histogram shows clearly equally spaced peaks, similar to the experimental histogram in Fig. 2*A*. (*B*) Histogram obtained by adding simulated force traces generated by a GMPCPP-MT bundle, corresponding to a zero catastrophe rate. Because the nucleation is high enough and there are no catastrophes, individual stalling events are observed much less frequently, which results in less obvious peaks in the histogram. (*Inset*) Example of such a force vs. time trace, showing no catastrophe and only stalling at the maximal force.